



A Multi-level Compression Scheme for Peak to Average Power Ratio Mitigation in SC-FDMA Communication System

Abbas Salman Hameed^{1*} Dheyaa T. Al-Zuhairi¹

¹*Department of Electronic, College of Engineering, University of Diyala, Diyala, Iraq*

* Corresponding author's Email: abbas_hameed_eng@uodiyala.edu.iq

Abstract: This paper proposes a peak to average power ratio (PAPR) reduction companding scheme for single carrier frequency division multiple access. The proposed technique has multi-level compression (MLC) stages where a signal is adjusted according to its instant value with respect to these levels. To validate MLC function, PAPR, bit error rate (BER), average power (P_{av}), and power spectral density (PSD) are evaluated through simulation. MLC improved PAPR significantly with low BER degradation. Using 16-QAM, MLC enhances PAPR by 4.38 dB while only 1.6 dB additional SNR is required to maintain 10^{-3} BER. MLC performance is compared with the recent companding techniques; Mu-law, Exponential, Trapezoidal, and tangent rooting. The BER simulation results show the superiority of MLC over these techniques. For PAPR reduction, different from other techniques, both Mu-law and MLC reduce PAPR significantly with close values. Finally, the Exponential and MLC preserve P_{av} with less side lobes in PSD.

Keywords: PAPR, SC-FDMA, Wireless communication, Signal compression.

1. Introduction

Single Carrier Frequency Division Multiple Access (SC-FDMA) system has been adopted in uplink 4th and 5th Generation wireless networks [1-3]. SC-FDMA offers several advantages, including minimal implementation complexity, and simplicity [3]. Another important merit for SC-FDMA is PAPR mitigation over orthogonal frequency division multiple access (OFDM). This what allows SC-FDMA to replace OFDM in uplink mobile communication [4].

The PAPR problem generation is summarized as follows: Fourier transform is an essential part in communication systems which transmit data as independent subcarriers. Generation of subcarriers in such a way usually produces some unwanted peaks in the signal. These peaks require large linear dynamic range for an efficient amplification. Consequently, increasing the cost and power consumption which are challenging issues for uplink units [5, 6]. To lessen the PAPR, these peaks should be processed before transmission.

Although of the PAPR reduction accomplishment achieved by SC-FDMA system, the research has not been halted keeping more PAPR mitigation in that system. There is a variety in the techniques which have been studied to deal with PAPR problem in SC-FDMA [4-16]. Among them, partial transmit sequence [4], pulse shaping [5], constellation extension [6], and selective mapping [7] were proposed. However, every one of these techniques suffers from noise increment, bandwidth expansion or additional complexity. Another method suggested in [8] achieved slight PAPR reduction for moderate error rate degradation at the receiver. Filters were also associated in SC-FDMA PAPR reduction [9]. Using filters could affect the in-band frequency components because every symbol time produced by Fourier transform contains a sum of discrete frequencies.

Due to their advantages, Companding techniques have been an attractive trend to solve PAPR problem in multicarrier communication systems [13-18]. Simplicity, bandwidth preserving along with the performance effectiveness are the merits of

Companding [13-18]. Different companding algorithms have been proposed for that purposed. Mu-law is a basic form of companding used for PAPR reduction. Mu-law strategy is increasing the low values of the signal and preserving the peaks with no change. Average power increment drives the signal over the linear limit of the power amplifier and consequently system performance degradation. K. Shri Ramtej and S. Anuradha suggested Exponential Companding (Exp) for PAPR enhancement [13]. In this Companding, P_{av} is kept the same and spectrum side lobes are lower than Mu. However, the complexity is still the main drawback of Exp [18]. Amal Fawzy et al. studied and compared between Exp, Cos, Tangent Rooting (tanhR) and Logarithmic Root Companding techniques [14]. It was found that tanhR outperformed the other techniques in BER for almost the same PAPR value. In [15], the performance of Rooting, Error function, Logarithmic and Exp companding algorithms were discussed. It was found that Exp has the best PAPR and BER performances over the others. Another companding technique based on approximating the magnitudes distribution of discrete cosine transform DCT-SC-FDMA was proposed in [16]. The main idea of this companding method is transforming the signal distribution to be triangular. Although PAPR is improved by this technique, it has high out of band PSD.

This article proposes a new companding technique to reduce PAPR in SC-FDMA. The main feature of the proposed technique is achieving significant PAPR reduction with low complexity. The SC-FDMA signal compression is realized using four carefully selected threshold levels. These levels are applied symmetrically on the positive and negative amplitudes of the signal. The signal values between the two internal levels are scaled, whereas the peaks are trimmed. Such levels distribution preserves the signal power with a negligible in-band distortion. As a result, the BER will not be much affected. At the receiver side and at a given time, the signal is reconstructed via decompressing process depending on the data value with respect to the same threshold levels.

The rest of this paper is arranged along these lines: Section 2 presents the typical SC-FDMA system as well as a short explanation of PAPR problem. Section 3 introduces the proposed MLC technique for PAPR reduction, while the simulated results are discussed in Section 4. Lastly, Section 5 lists the most important conclusion points.

2. SC-FDMA system and PAPR problem

This section includes two parts: the structure of SC-FDMA system and PAPR problem. Fig. 1 shows the transceiver of SC-FDMA where the input data bits are mapped on constellation according to the used modulation type. The obtained symbols are divided into blocks of size N . Then the N symbols enter in parallel form to the DFT stage. DFT converts the data to frequency domain samples as [19, 20]:

$$X(l) = \frac{1}{\sqrt{N}} \sum_{n=0}^{N-1} d(n) e^{-j\frac{2\pi ln}{N}} \quad (1)$$

where $d(n), n = 0, 1, \dots, N-1$, is the data of each block, $X(l), l = 0, 1, \dots, N-1$, is the vector representing the frequency domain samples.

The subcarrier mapping determines the SC-FDMA mapping type to be interleaved (IFDMA), Localized (LFDMA), or Distributed (DFDMA). Generally, zeros are padded and used along with $X(l)$ as input to the M -point inverse discrete Fourier transform (IDFT) to form M subcarriers, where $M > N$. The difference between the mapping types is the mechanism of arranging the frequency domain samples positions with the zeros as follows. In IFDMA, the mapping can be written as [20]:

$$Q(p) = \begin{cases} X(l), & \text{where } p = lP \\ 0, & \text{otherwise} \end{cases} \quad (2)$$

where Q is the mapped vector of length M and P is number of sub-channels given by M/N .

For LFDMA, the $X(l)$ elements are packed in consecutive subcarriers as [20]:

$$Q(p) = \begin{cases} X(l), & \text{where } p = l \\ 0, & \text{otherwise} \end{cases} \quad (3)$$

Whereas in DFDMA, the frequency domain samples, X , are spread within a lower number of sub-channels than in IFDMA. Hence, the Q elements of DFDMA can be defined as:

$$Q(p) = \begin{cases} X(l), & \text{where } p = l\tilde{P} \\ 0, & \text{otherwise} \end{cases} \quad (4)$$

where \tilde{P} is the number of DFDMA sub-channels and should be less than P .

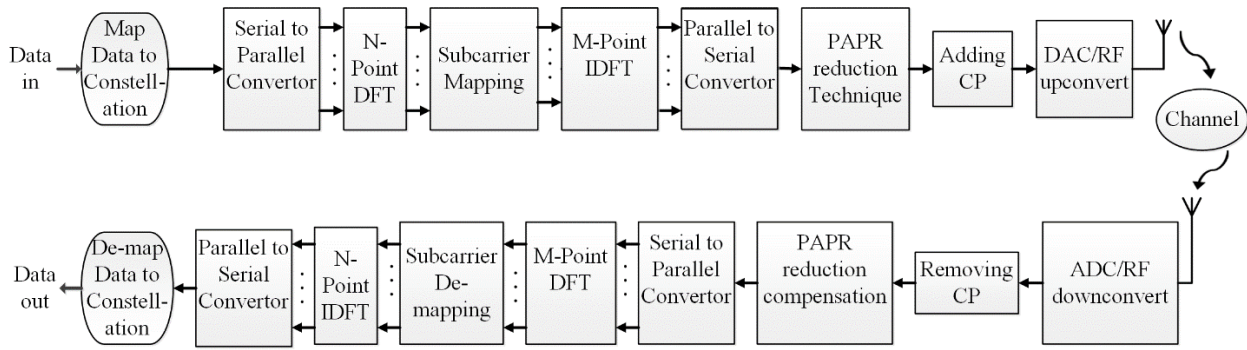


Figure. 1 SC-FDMA with PAPR reduction

After that, the Q mapped vector is processed using M -point IDFT as follows [5, 21]:

$$B(k) = \frac{1}{\sqrt{M}} \sum_{m=0}^{M-1} Q(m) e^{j\frac{2\pi km}{M}} \quad (5)$$

where $k = 0, 1, \dots, M - 1$.

Parallel to serial converter is used to convert B into serial stream. Usually, a PAPR reduction technique is inserted at the transmitter side to mitigate the data distortion and power consumption. Finally, after adding Cyclic Prefix (CP), the signal is converted to analogue and up converted to RF frequency for transmitting.

Through the channel, Additive White Gaussian Noise (AWGN) is added to the transmitted signal $s(t)$. Thus, the received signal is:

$$r(t) = s(t) \otimes h(t) + n_w(t) \quad (6)$$

where $h(t)$ is the channel impulse response and $n_w(t)$ is AWGN.

At the receiver side, all the processes which took place at transmitter side are inverted to obtain the reconstructed data $\hat{d}(n), n = 0, 1, \dots, N - 1$.

Before signal transmission, the signal needs to be amplified using a power amplifier. For wireless uplink connection, two important points should be implied which are the efficiency of the amplification and the battery life of the user equipment [22]. Due to the linear combination of random symbols at the IFFT in the transmitter side, high peaks most likely occur at the output compared to the average of the signal. This phenomenon is known as PAPR. The linearity range of the amplifier is limited, and working outside this range leads to distort the amplified signal. Therefore, a technique must be used to reduce PAPR and maintain the efficient amplification of the power amplifier [22, 23].

One criterion for evaluating communication systems performance is PAPR which can be expressed mathematically by [21, 24]:

$$PAPR = 10 \log_{10} \frac{\max(|B|^2)}{E(|B|^2)} \quad (7)$$

where $E(\cdot)$ represents the expectation value.

The PAPR is usually evaluated by its Complementary Cumulative Distribution Function (CCDF) which can be defined as the PAPR probability of SC-FDMA symbol over the threshold PAPR (γ) value [21]. Mathematically, $CCDF(\gamma)$ is given by [21, 23]:

$$CCDF(\gamma) = 1 - (1 - e^{-\gamma})^{2.8M} \quad (8)$$

3. Proposed multi-level compression technique (MLC)

This section introduces our proposed technique for PAPR reduction in SC-FDMA communication system. In this method, the signal samples are modified after IDFT stage at the transmitter side. MLC PAPR reduction technique considers both the absolute and phase of the IDFT output signal which are the vectors $|B|$ and θ_1 , respectively. Because the amplitude is the source of PAPR problem, the process includes the absolute only while the phase is preserved to be added later before CP insertion.

Vector $|B|$ is pre-processed as follows:

$$H = |B| - V1 \quad (9)$$

where $V1$ is the mean of $|B|$.

Then, the whole range of signal H is divided up by applying four threshold levels ($Th_{1lo}, Th_{2lo}, Th_{1up}$, and Th_{2up}) as shown in Fig. (2). Hence, there are five different parts on signal H in that figure as follows:

- 1- Values of H less than or equal to Th_{1lo} .
- 2- Values of H less than or equal to Th_{2lo} and larger than Th_{1lo} .
- 3- Values of H less than or equal to Th_{1up} and larger than Th_{2lo} .
- 4- Values of H less than Th_{2up} and larger than or equal to Th_{1up} .

5- Values of H larger than or equal to Th_{2up} .

Each part is compressed individually according to Eq. (10) and as shown in Fig. 2. At a given time index, i , the scaled output $H_c(i)$ is:

$$H_c(i) = \begin{cases} Out_{1lo}, & \text{for } H(i) \leq Th_{1lo} \\ Out_{2lo}, & \text{for } Th_{1lo} < H(i) \leq Th_{2lo} \\ \frac{Out_{2up}}{Th_{2up}} H(i), & \text{for } Th_{2lo} < H(i) < Th_{1up} \\ Out_{1up}, & \text{for } Th_{1up} \leq H(i) < Th_{2up} \\ Out_{2up}, & \text{for } H(i) \geq Th_{2up} \end{cases} \quad (10)$$

where Out_{1lo} , Out_{2lo} , Out_{1up} , and Out_{2up} are the output compression values selected with respect to the threshold levels.

Finally, the phase is returned back after adding the mean of $|B|$ to vector H_c and the result signal can be expressed as:

$$S_c = (H_c + V1)e^{j\theta1} \quad (11)$$

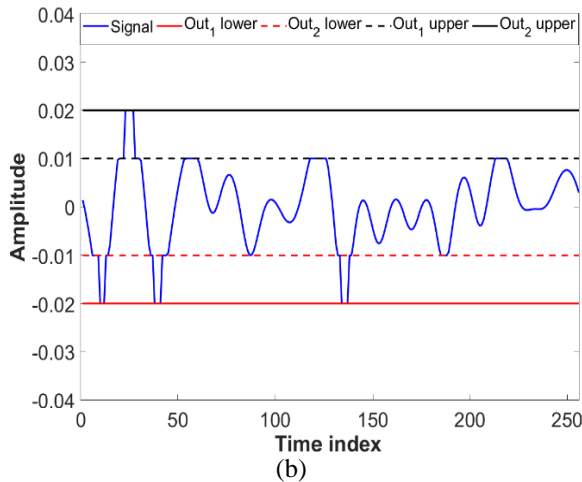
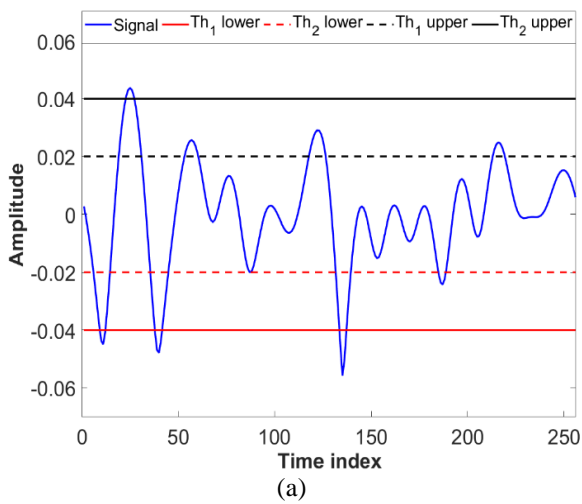


Figure. 2 Signal with MLC threshold levels: (a) before compressing and (b) after compressing

The PAPR is reduced now in S_c signal and thus the process related to the PAPR problem is finished at the transmitter side.

At the receiver side, the proposed process is inverted, and the compensation for PAPR reduction procedure is implemented after removing CP directly. Again, the signal absolute $|Z|$ and phase $\theta2$ are separated from each other and the process is conducted on the absolute only. The decompression starts from subtracting the mean from the signal to obtain the zero mean \tilde{S}_c signal as:

$$\tilde{S}_c = |Z| - V2 \quad (12)$$

where $V2$ is the mean of Z .

After that, the signal at a given time, i , can be decompressed using the following equation:

$$\tilde{H}_c(i) = \begin{cases} Th_{1lo}, & \text{for } \tilde{S}_c(i) \leq Out_{1lo} \\ Th_{2lo}, & \text{for } Out_{1lo} < \tilde{S}_c(i) \leq Out_{2lo} \\ \frac{Th_{2up}}{Out_{2up}} \tilde{S}_c(i), & \text{for } Out_{2lo} < \tilde{S}_c(i) < Out_{1up} \\ Th_{1up}, & \text{for } Out_{1up} \leq \tilde{S}_c(i) < Out_{2up} \\ Th_{2up}, & \text{for } \tilde{S}_c(i) \geq Out_{2up} \end{cases} \quad (13)$$

Finally, the mean $V2$ is added back to \tilde{H}_c and the reconstructed signal is acquired by merging the absolute and phase as follows:

$$\tilde{B} = (\tilde{H}_c + V2)e^{j\theta2} \quad (14)$$

Fig. 3 depicts the decompressed signal resulting from Eqs. (12) to (14) at the receiver.

4. Simulation results

This section presents and discuss the simulation numerical results of MLC technique for PAPR

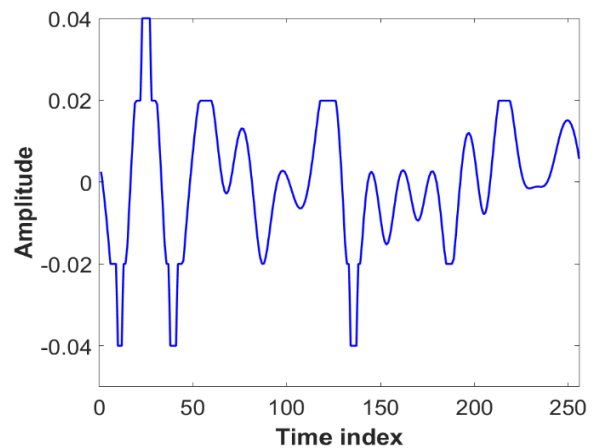


Figure. 3 Decompressed signal

Table 1. Simulation system parameters

Parameter	Value
simulation iteration number	10000
N	16
M	256
Modulation type	QPSK and 16-QAM
Channel model	Rayleigh and AWGN
Channel estimation	Ideal
System bandwidth	5 MHz
Subcarriers spacing	19.53125 kHz

reduction in SC-FDMA system. The simulation was implemented using MATLAB software. The SC-FDMA system simulation parameters are listed in Table 1.

To assess the effectiveness of any PAPR mitigation method, two criteria should be considered: CCDF and BER. Some methods reduce PAPR in cost of severe BER degradation. For a successful PAPR reduction technique, the important point is improving the CCDF and maintaining BER level as much as possible.

For MLC, the effect of the threshold levels selection on PAPR and BER is tested first. Then, the performance is compared with some well-known PAPR reduction methods.

The values of threshold levels depend on the modulation type. To select the best levels values, the lower threshold levels were changed with keeping the upper ones, then fixing the lower levels and varying the upper ones. For QPSK modulation, the tested pairs of (Th_{1lo}, Th_{2lo}) were Pair1 = $(-0.06, -0.04)$, Pair2 = $(-0.04, -0.02)$ and Pair3 = $(-0.02, -0.01)$. Fig. 4(a) and 4(b) illustrate the effect of changing the aforementioned pairs of lower threshold levels on PAPR and BER, respectively. In both figures, Pair2 represents the compromise choice for PAPR and BER performances. For the same modulation type, Pair1 = $(0.04, 0.06)$, Pair2 = $(0.02, 0.04)$ and Pair3 = $(0.01, 0.02)$ were the candidate pairs for the right (Th_{1up}, Th_{2up}) selection. The trade-off performance is obtained from Pair2. Fig. 5(a) and 5(b) depict the effect of changing the upper threshold levels on PAPR and BER, respectively. The same way for 16-QAM, the best pairs of (Th_{1lo}, Th_{2lo}) and (Th_{1up}, Th_{2up}) were found to be $(-0.12, -0.07)$ and $(0.07, 0.12)$, respectively.

The effectiveness of MLC needs to be evaluated in comparison with some of the familiar companding PAPR reduction techniques; Mu-law, Exp, trapezoidal (Trap) [17] and tanhR. Depending on the used PAPR reduction scheme, the average

signal power may or may not increase. To avoid the nonlinear distortion, a PAPR reduction scheme should keep a constant average signal power. Table 2 shows the signal power average before and after applying all the foregoing techniques and MLC on SC-FDMA system. The values in the table declare that P_{av} is preserved in both Exp and MLC, while P_{av} value is significantly changed in Mu-law, Trap, and tanhR techniques. For instant, at LFDMA QPSK scenario, the P_{av} increment were 164%, 307%, and 230% for Mu-law, Trap, and tanhR respectively compared with P_{av} in case of no PAPR reduction technique used.

Respecting the modulation type effect on PAPR reduction techniques, Fig. 6 and 7 show the LFDMA performance under QPSK and 16-QAM. For QPSK, Fig. 6 illustrates the effect of using PAPR reduction techniques on mitigation PAPR problem. At 10^{-3} CCDF, this figure depicts that MLC technique outperforms Mu-law, Exp, Trap, and tanhR techniques by 0.32 dB, 1.1 dB, 1.05 dB, 1.36 dB,

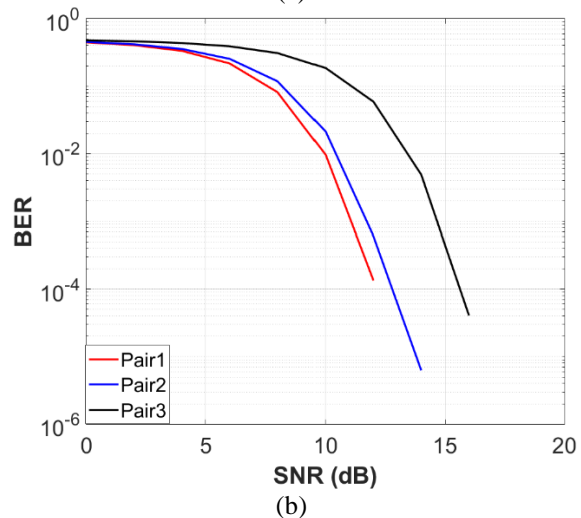
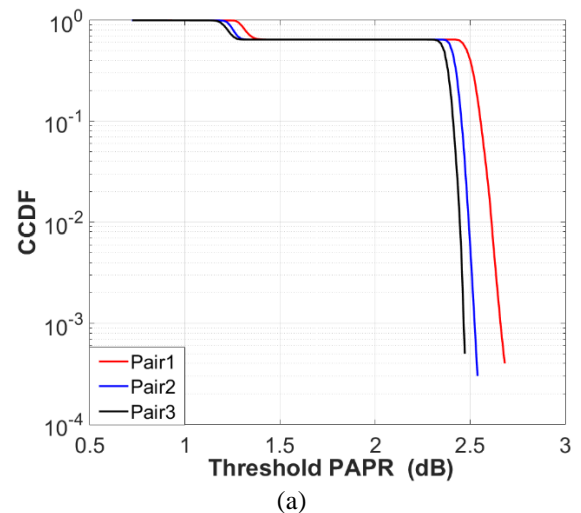


Figure. 4 System performance for different lower threshold levels: (a) PAPR and (b) BER

Table 2. Average power before and after applying PAPR reduction techniques

Technique		LFDMA QPSK	LFDMA 16QAM	DFDMA QPSK	DFDMA 16QAM
Average Power without ($P_{without}$)		0.0039	0.0468	0.0039	0.0429
Mu-law	Average power (P_{Mu})	0.0064	0.0987	0.0082	0.0735
	$P_{Mu}/P_{without}$	164%	211%	210%	171%
Exp [11]	Average power (P_{Exp})	0.0039	0.0468	0.0039	0.0429
	$P_{Exp}/P_{without}$	100%	100%	100%	100%
Trap [17]	Average power (P_{Trap})	0.012	0.0122	0.0123	0.0101
	$P_{Trap}/P_{without}$	307%	26%	315%	22%
tanhR [12]	Average power (P_{tanhR})	0.009	0.54	0.009	0.547
	$P_{tanhR}/P_{without}$	230%	1148%	230%	1275%
MLC	Average power (P_{Pro})	0.0037	0.0455	0.0037	0.0413
	$P_{Pro}/P_{without}$	95%	97%	95%	96%

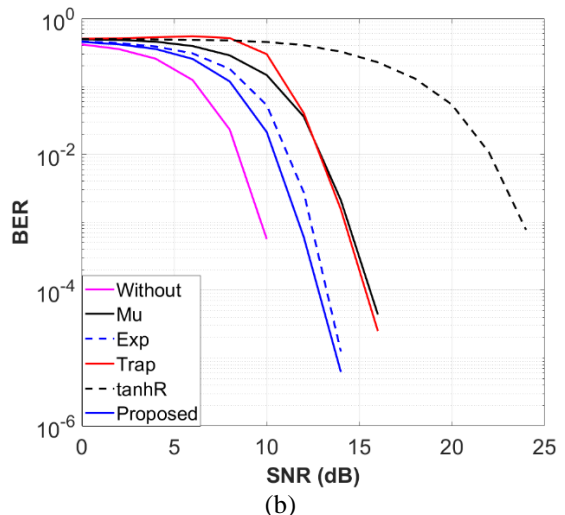
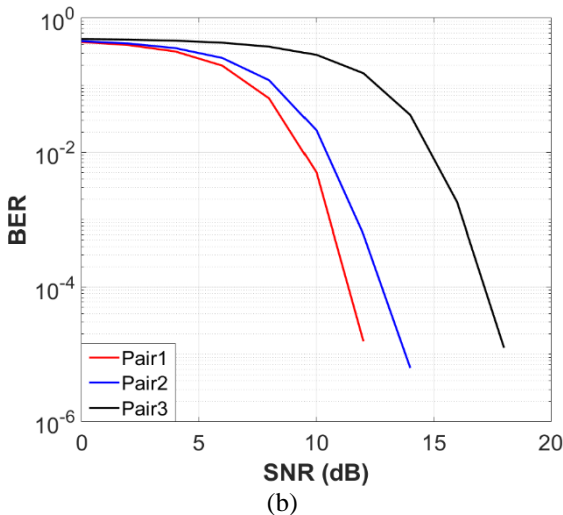
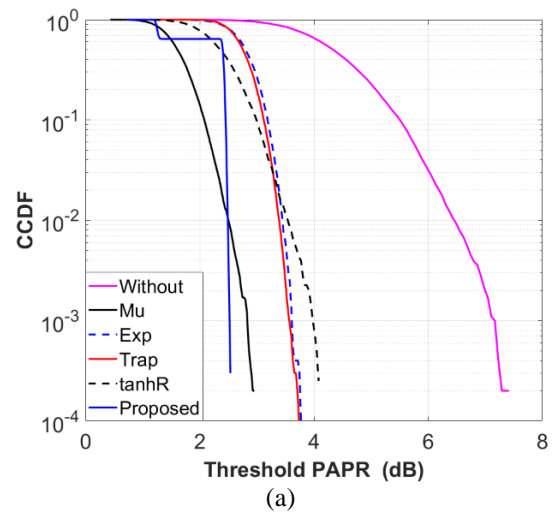
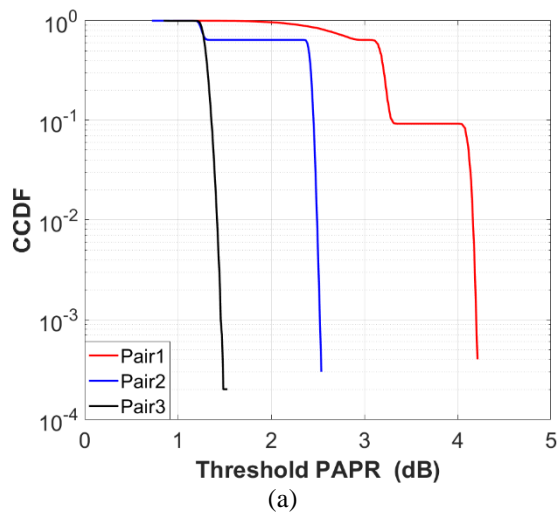


Figure. 5 System performance for different upper threshold levels: (a) PAPR and (b) BER

Figure. 6 Performance comparison of QPSK LFDMA with different PAPR reduction techniques: (a) CCDF and (b) BER

respectively. In the same view, the reduction in PAPR was 4.65 dB using MLC technique compared with no technique. PAPR reduction is usually in expense of BER degradation.

However, Fig. 6 shows the superiority of MLC over the other techniques in BER performance.

There are 0.7 dB, 2.7 dB, 2.5 dB, 9.7 dB SNR saving using MLC compared with Mu-law, Exp, Trap, and tanhR, respectively. The same comparison is conducted for 16-QAM. At 10^{-3} CCDF, Mu-law

Table 3. Comparison between PAPR reduction techniques for SC-FDMA

Technique		LFDMA QPSK	LFDMA 16QAM	DFDMA QPSK	DFDMA 16QAM
PAPR (dB) at CCDF = 10^{-3}	Without	7.17	7.79	7.16	7.79
	Mu-law	2.84	3.27	2.83	3.27
	Exp	3.62	4.16	3.61	4.16
	Trap	3.57	4.9	3.5	4.95
	tanhR	3.88	4.91	3.74	4.81
	MLC	2.52	3.41	2.52	3.41
SNR (dB) at BER = 10^{-3}	Without	9.7	19	9.28	18.13
	Mu-law	14.4	No value	15.38	No value
	Exp	12.4	23.6	12.38	23.71
	Trap	14.2	No value	15.5	No value
	tanhR	21.4	No value	21.78	No value
	MLC	11.7	20.6	11.53	20.7

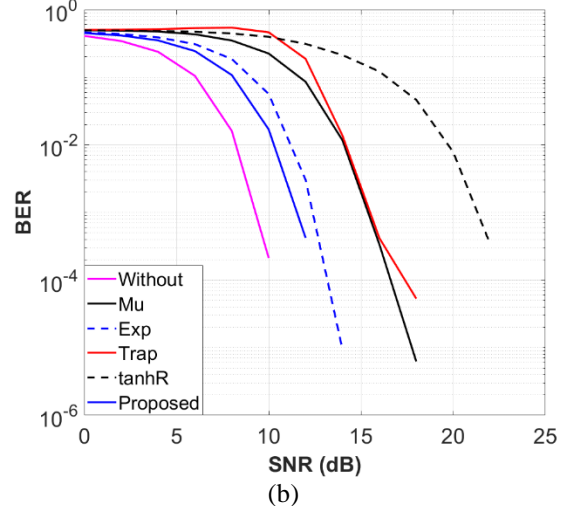
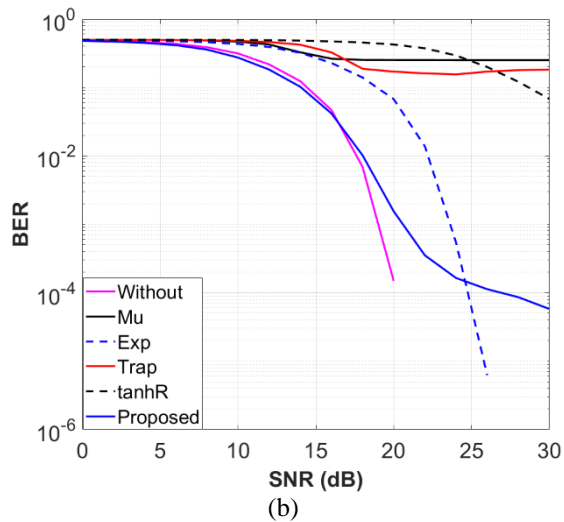
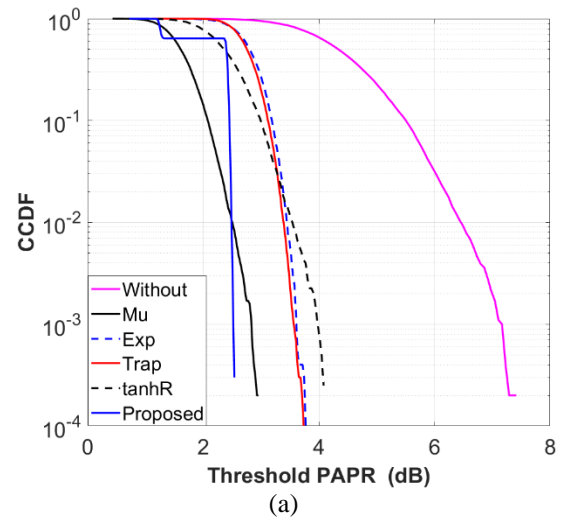
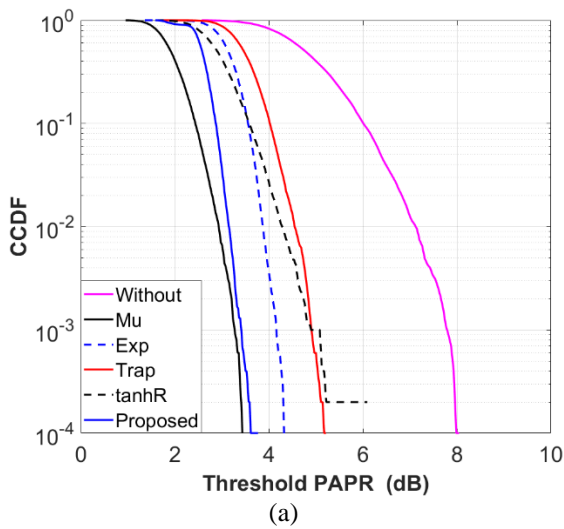


Figure 7 Performance comparison of 16-QAM LFDMA with different PAPR reduction techniques: (a) CCDF and (b) BER

Figure 8 Performance comparison of QPSK DFDMA with different PAPR reduction techniques: (a) CCDF and (b) BER

companding records slight superiority in PAPR reduction performance with only 0.14 dB better than MLC as shown in Fig. 7. However, the system with Mu-law loses the ability of correctly data detection

and produces a relatively constant unacceptable BER value as shown in Fig. 7.

The results of DFDMA system are not far away from those of LFDMA. Fig. 8 and 9 depict the PAPR reduction techniques performance in

DFDMA system for QPSK and 16-QAM, respectively. Detailed numerical results are tabulated in Table 3 as a performance comparison between the tested PAPR reduction techniques.

PSD is another factor which reflects the performance of PAPR reduction techniques. In addition to MLC excellence in CCDF and BER performance over the other schemes, Fig. 10 shows the supremacy of MLC over the other companding schemes in term of PSD out of signal band except Exp companding which has little bit weaker PSD over MLC. For comparison, the PSD is averaged for 2 MHz out of the transmission band for the SC-FDMA system without PAPR reduction technique, using Mu-law, Exp, Trap, tanhR and MLC companding techniques. Whereas the average PSD of the system without using any PAPR reduction technique was -36.15 dB, the average PSD were -31.88 dB, -35.63 dB, -34.11 dB, -31.45 dB

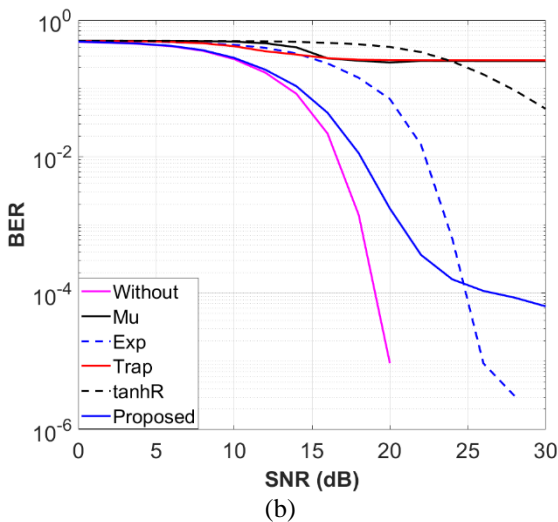
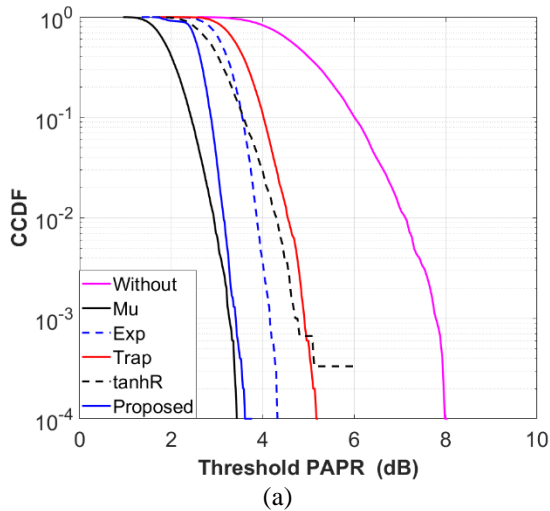


Figure. 9 Performance comparison of 16-QAM DFDMA with different PAPR reduction techniques: (a) CCDF and (b) BER

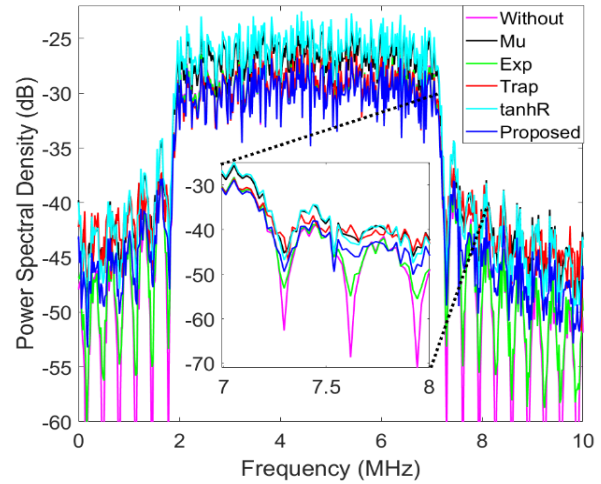


Figure. 10 Power spectral density of the PAPR reduction technique

and -35.17 dB for Mu-law, Exp, Trap, tanhR and MLC techniques respectively.

It is worth to mention that both Mu-law and tanhR companding techniques have the worst PSD and, that is because they increase the signal average significantly as shown earlier in Table 2. Due to increasing the signal average using these techniques, a power amplifier with a larger linearity range is required for the system. Otherwise, increasing the signal average leads to more bit errors at the receiver.

After all, the performance of the proposed MLC and Exp companding illustrates the superiority over the other companding techniques in terms of CCDF, BER, and PSD. However, there is another essential factor in the comparison which is the technique complexity. The exponential function in the Exp companding makes it more complex compared with MLC technique. This point is considered as another merit for MLC technique.

5. Conclusion

In this paper, a multi-level compression scheme called MLC is proposed to mitigate PAPR problem in SC-FDMA system. MLC divides signal into five parts according to the scheme threshold levels. Every part of the signal is processed separately. The threshold levels were selected carefully depending on the modulation type for better performance. Processing signals with MLC technique maintains its average power while reduces the signal peaks. Both LFDMA and DFDMA systems are included in the simulation. The metrics CCDF, BER, PSD and P_{av} are considered for the comparison between the performances of Mu-law, Exp, Trap, tanhR and MLC companding schemes. For QPSK LFDMA and at 10^{-3} CCDF, the system without using any PAPR

reduction technique records PAPR of 7.17 dB, though the values are 2.84 dB, 3.62 dB, 3.57 dB, 3.88 dB and 2.52 dB for Mu-law, Exp, trap, tanhR and MLC, respectively. For 16-QAM, the system with no PAPR reduction technique gets PAPR of 7.79 dB, whereas the values are 3.27 dB, 4.16 dB, 4.9 dB, 4.91 dB and 3.41 dB for Mu-law, Exp, trap, tanhR and MLC techniques, respectively. Moreover, MLC outperforms the others in BER comparison. At 10^{-3} BER, MLC scheme improved SNR by at least 3 dB over the other schemes for both QPSK and 16-QAM. The Exp technique achieves an insignificant advantage respecting PSD over the proposed technique, however it is a much higher complexity approach.

Conflicts of Interest

The authors declare no conflict of interest.

Author Contributions

All the paper work including conceptualization, methodology, validation, formal analysis, writing—original draft preparation, writing—review and editing were prepared by the two authors equally.

References

- [1] A. Li, A. Benjebbour, X. Chen, H. Jiang, and H. Kayama, “Uplink Non-Orthogonal Multiple Access (NOMA) with Single-Carrier Frequency Division Multiple Access (SC-FDMA) for 5G systems”, *IEICE Transactions on Communications*, Vol. E98B, No. 8, pp. 1426-1435, 2015.
- [2] O. ylipisto and Institute of Electrical and Electronics Engineers, “5G New Radio EVolution Towards Sub-THz Communications”, In: *Proc. of 2nd 6G Wireless Summit conf. 2020*, pp. 1-6, 2020.
- [3] D. Na, S. Jang, W. G. Seo, and K. Choi, “Field Trials of SC-FDMA, FBMC and LP-FBMC in IndoorSub-3.5 GHz Bands”, *Electronics*, Vol. 10, No. 5, pp. 1-15, 2021.
- [4] N. A. Moghaddam, A. Maleki, and A. R. Sharafat, “Peak-to-average power ratio reduction in LTE-advanced systems using low complexity and low delay PTS”, *IET Communications*, Vol. 14, No. 11, pp. 1768-1772, 2020.
- [5] J. Ji, G. Ren, and H. Zhang, “PAPR Reduction of SC-FDMA Signals Via Probabilistic Pulse Shaping”, *IEEE Transactions on Vehicular Technology*, Vol. 64, No. 9, pp. 3999-4008, 2015.
- [6] H. Y. Liang and H. C. Chu, “Improving the peak-to-average power ratio of single-carrier frequency division multiple access systems by using an improved constellation extension scheme with error correction”, *Telecommunication Systems*, Vol. 65, No. 3, pp. 377-386, 2017.
- [7] H. Sakran, “An efficient joint algorithm for reducing PAPR of SC-FDMA system in cognitive radio networks”, *Wireless Networks*, Vol. 25, No. 3, pp. 1117-1124, 2019.
- [8] K. Wu, G. Ren, and M. Yu, “PAPR Reduction of SC-FDMA Signals Using Optimized Additive Pre-distortion”, *IEEE Communications Letters*, Vol. 19, No. 8, pp. 1446-1449, 2015.
- [9] Y. U, F. Wang, and J. Lu, “Low PAPR Filter Bank Single Carrier for 5G mMTC”, *IEEE Internet of Things Journal*, Vol. 6, No. 4, pp. 6887-6895, 2019.
- [10] D. Sinanović, G. Šišul, A. S. Kurdija, and Ž. Ilić, “Multiple transmit antennas for low PAPR spatial modulation in SC-FDMA: single vs. multiple streams”, *Eurasip Journal on Wireless Communications and Networking*, Vol. 2020, No. 1, 2020.
- [11] A. M. Musa, R. A. Mokhtar, R. A. Saeed, H. Alhumyani, S. A. Khalek, and A. O. Y. Mohamed, “Distributed SC-FDMA sub-carrier assignment for digital mobile satellite”, *Alexandria Engineering Journal*, Vol. 60, No. 6, pp. 4973-4980, 2021.
- [12] H. Lu, Y. Zhou, Y. Liu, R. Li, and N. Cao, “PAPR Reduction Scheme for Localized SC-FDMA Based on Deep Learning”, In: *Proc. of International Conference on Wireless and Satellite Systems*, pp. 697-708, 2019.
- [13] K. S. Ramtej and S. Anuradha, “Exponential Companding Transform to Mitigate PAPR in SC-FDMA Systems”, In: *Proc. of Photonics & Electromagnetics Research Symposium-Spring*, pp. 4174-4179, 2019.
- [14] A. F. A. E. Rahman, “Companding techniques for SC-FDMA and sensor network applications”, *International Journal of Electronics Letters*, Vol. 8, No. 3, pp. 241-255, 2020.
- [15] K. S. Ramtej and S. Anuradha, “On companding techniques to mitigate PAPR in SC-FDMA systems”, *International Journal of Wireless and Mobile Computing*, Vol. 18, No. 3, pp. 295-302, 2020.
- [16] S. R. Kondamuri and A. Sundru, “Non Linear Companding Transform to Mitigate PAPR in DCT Based SC-FDMA System”, *Wireless*

- Personal Communications*, Vol. 112, No. 1, pp. 503-522, 2020.
- [17] S. Gupta and A. Goel, "Generalized Trapezoidal Companding Technique for PAPR Reduction in OFDM Systems", *Journal of Optical Communications*, Vol. 42, No. 2, pp. 341-349, 2021.
- [18] S. S. Jeng, J. M. Chen, and P. H. Chang, "A low-complexity companding technique using Padé approximation for PAPR reduction of an OFDM system", *International Journal of Communication Systems*, Vol. 24, No. 11, pp. 1467-1479, 2011.
- [19] J. S. Roy and S. Mishra, "Performance of SC-FDMA for LTE Uplink Under Different Modulation Schemes", In: *Proc. of International Conference on Mechatronics, Robotics and Systems Engineering*, pp. 202-206, 2019.
- [20] S. Kumar, M. S. Chaudhari, R. Gupta, and S. Majhi, "Multiple CFOs Estimation and Implementation of SC-FDMA Uplink System Using Oversampling and Iterative Method", *IEEE Transactions on Vehicular Technology*, Vol. 69, No. 6, pp. 6254-6263, 2020.
- [21] D. J. G. Mestdagh, J. L. G. Monsalve, and J. M. Brossier, "GreenOFDM: A new selected mapping method for OFDM PAPR reduction", *Electronics Letters*, Vol. 54, No. 7, pp. 449-450, 2018.
- [22] H. Asplund, V. B. P. Astely, T. Chapman, M. Frenne, F. Ghasemzadeh, and E. Larsson, "Advanced Antenna Systems for 5G Network Deployments Bridging the Gap Between Theory and Practice, 1st edition", *Academic Press*, 2020.
- [23] X. Liu, L. Zhang, J. Xiong, X. Zhang, L. Zhou, and J. Wei, "Peak-to-Average Power Ratio Analysis for OFDM-Based Mixed-Numerology Transmissions", *IEEE Transactions on Vehicular Technology*, Vol. 69, No. 2, pp. 1802-1812, 2020.
- [24] M. I. A. Rayif, H. E. Seleem, A. M. Ragheb, and S. A. Alshebeili, "PAPR Reduction in UFMC for 5G Cellular Systems", *Electronics*, Vol. 9, No. 9, pp. 1-15, 2020.